Electronic Supplementary Material (ESI) for Green Chemistry.

Supporting Information

Solvent-free synthesis of morphology-controllable nickel sulfides in one-pot plasma reactions for high-performance lithium-ion batteries

Yinghui Yang,[a] *Junzhang Wang,*[a] *Chao Wang,*[a] *Rongzhang Guan,*[a] *Dujiang Lu,*[a] *Shuchun Zhao,*[b] *Shuai Liu,*[a] *and Xiufang Bian**[a]

[a] Key Laboratory for Liquid-Solid Evolution and Processing of Materials (Ministry of Education), School of Materials Science and Engineering, Shandong University, Jinan 250061, China.

[b] Center of Electron Microscopy and State Key Laboratory of Silicon Materials, School of Materials Science & Engineering, Zhejiang University, Hangzhou 310027, China

* Corresponding author. E-mail address: xfbian@sdu.edu.cn

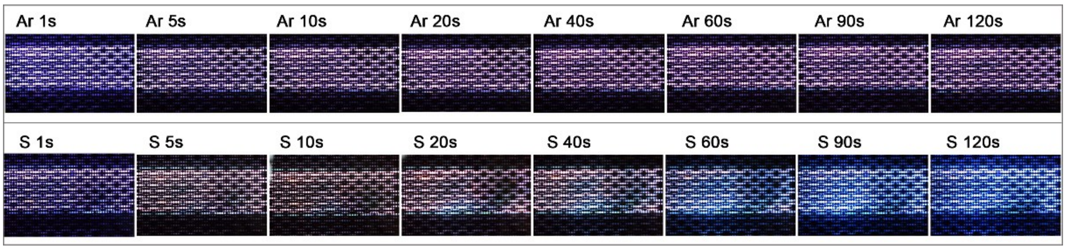

Fig. S1. The color change over time of Ar-plasma and S-plasma.

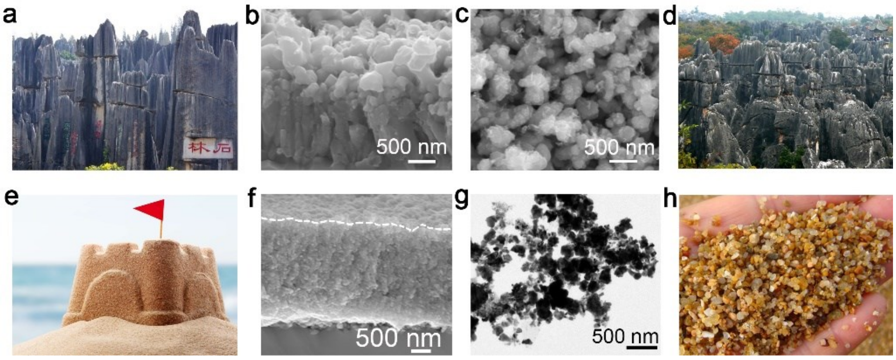

Fig. S2. The comparative figure. (a) The photograph of stone forest taken at a parallel height. (b) The SEM image of the cross-section of SF-NS. (c) The SEM image of the surface of SF-NS. (d) The photograph of stone forest taken at a high height. (e) The photograph of a castle-like sandpile. (f) The SEM image of the cross-section of SP-NS. (g) The TEM image of the nanoparticles in SP-NS. (h) The photograph of sand.

The stone forest is an array of irregular stone columns with rocks on the top, just like the columnar nickel sulfides covered by blocky nickel sulfides in SF-NS. There is space between the stone column in stone forest. Similarly, there is space between nickel sulfides in SF-NS.

SP-NS is a stack of irregular nickel sulfides nanoparticles that are similar with sand. Due to the low integration of structure, the nickel sulfides nanoparticles peeled off during electrochemistry reaction. The structural instability of SF-NS is also similar to sandpile.

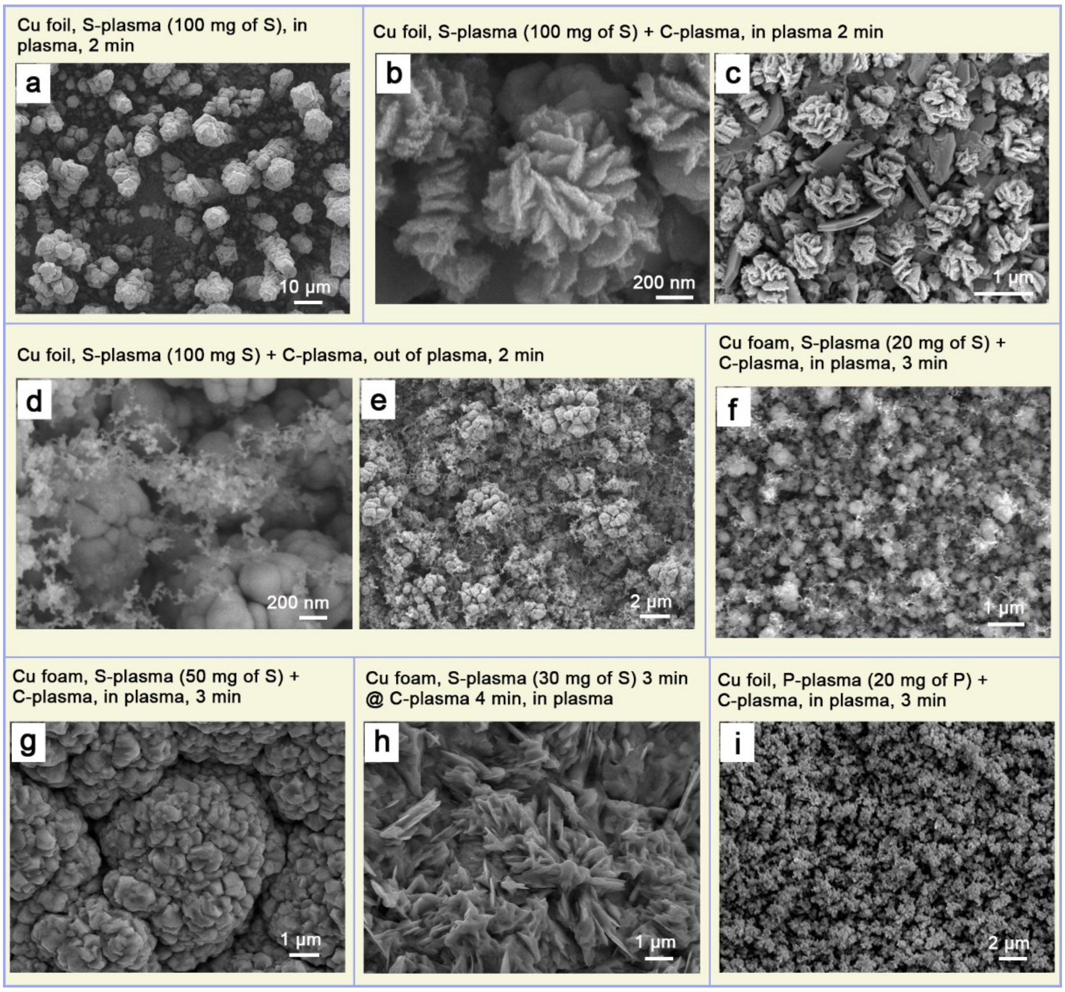

Fig. S3. The morphology-controllable copper sulfides and copper phosphides synthesized in microwave plasma sulfidation method. (a) Tower-like copper sulfides. (b, c) Desert-rose-stone-like copper sulfides. (d-f) Walnut-like copper sulfides. (g) Cauliflower-like copper sulfides. (h) Lichen-like copper sulfides. (i) Copper phosphides.

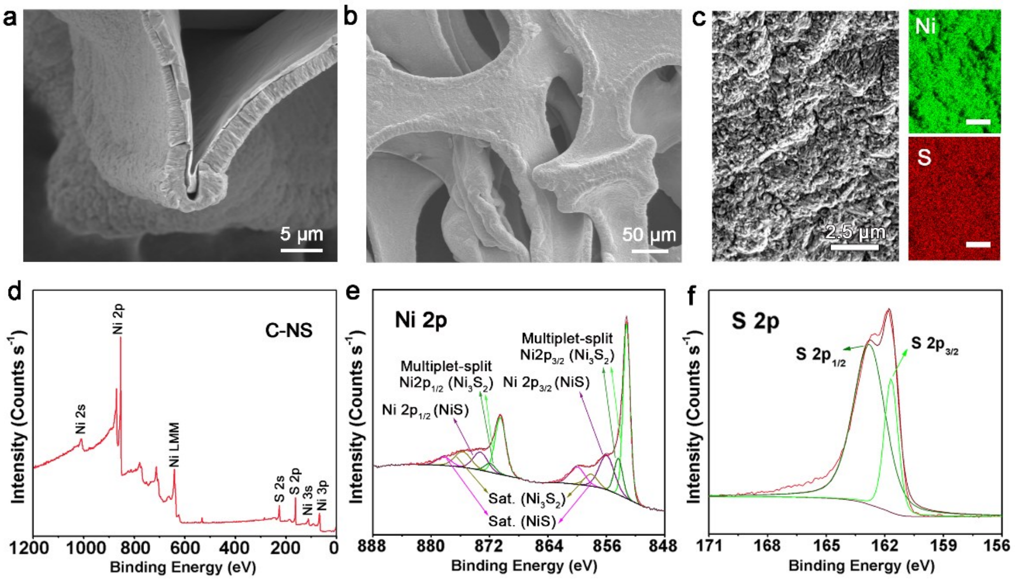

Fig. S4. The characteristics of C-NS. The cross-section morphology (a) and surface morphology (b) of C-NS after 2 min at low magnification. (c) The EDS mappings at the surface of C-NS. The scales are 2.5 μm. (d) The XPS survey spectrum of C-NS. (e) The XPS high-resolution spectrum of Ni 2p. (f) The XPS high-resolution spectrum of S 2p.

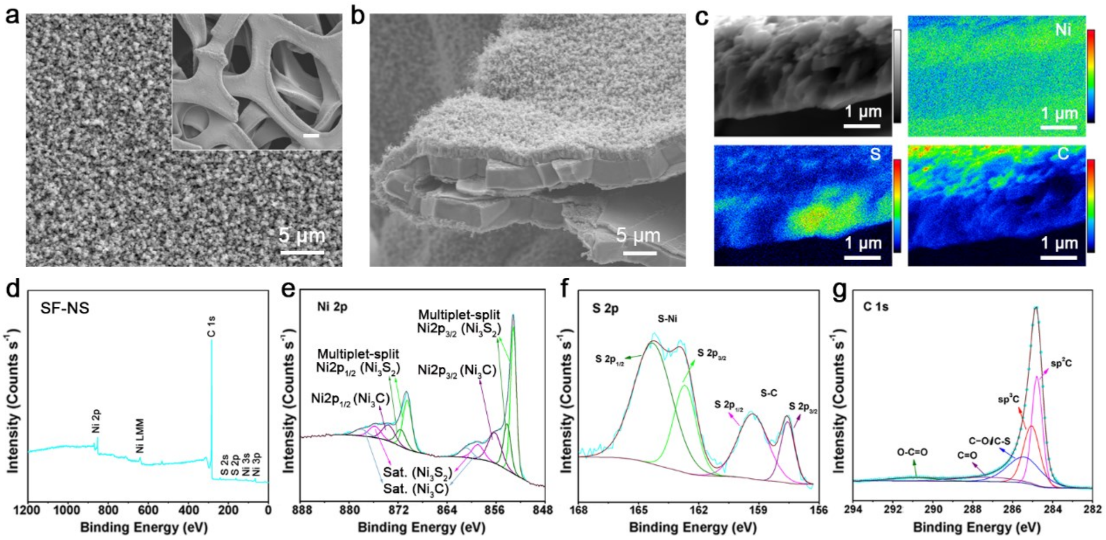

Fig. S5. The characteristics of SF-NS. The SEM images of the top surface (a) and cross-section (b) of SF-NS at low magnification. The scale in the inset of (a) is 50 μm. (c) The EPMA mappings of the cross-section of SF-NS. (d) The XPS survey spectrum of SF-NS. (e) The XPS high-resolution spectrum of Ni 2p. (f) The XPS high-resolution spectrum of S 2p. (g) The XPS high-resolution spectrum of C 1s.

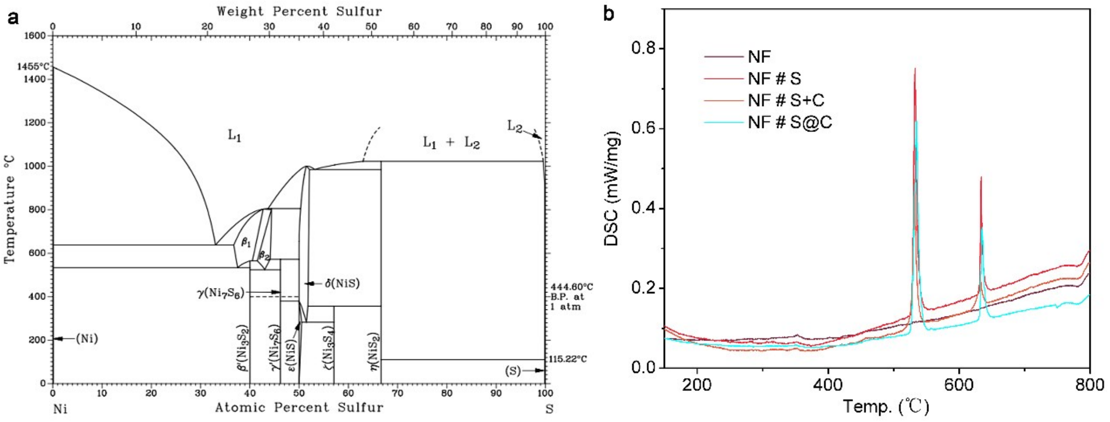

Fig. S6. (a) The phase diagram of nickel-sulfur alloy. (b). The DSC spectra of nickel foam, C-NS, SF-NS and SP-NS.

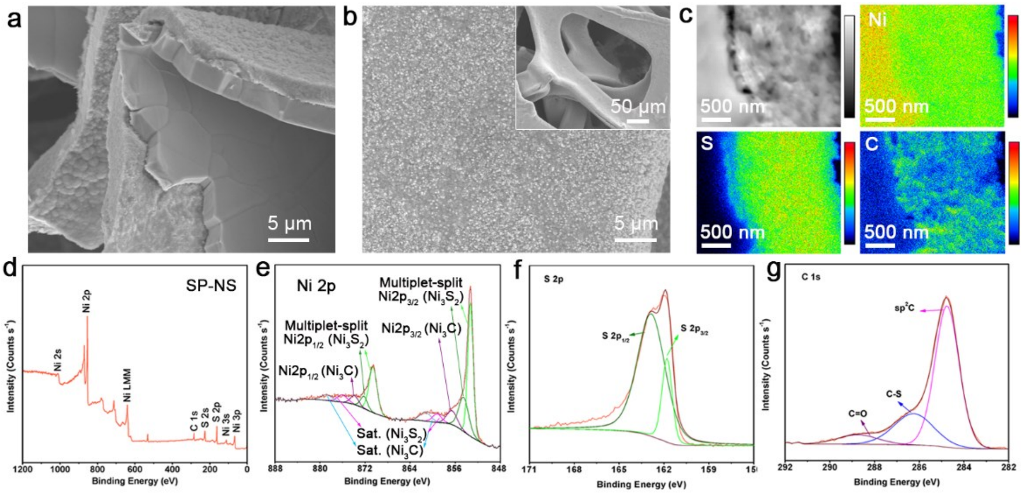

Fig. S7. The characteristics of SP-NS. The SEM images of the cross-section (a) and top surface (b) of SP-NS at low magnification. (c) The EPMA mappings of the cross-section of SP-NS. (d) The XPS survey spectrum of SP-NS. (e) The XPS high-resolution spectrum of Ni 2p. (f) The XPS high-resolution spectrum of S 2p. (g) The XPS high-resolution spectrum of C 1s.

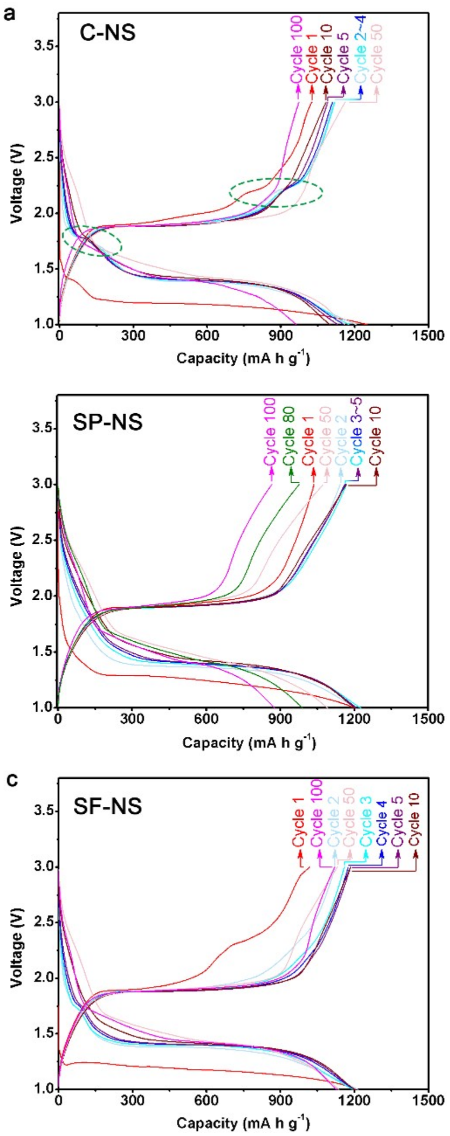

Fig. S8. The voltage platforms of (a) C-NS, (b) SP-NS and (c) SF-NS.

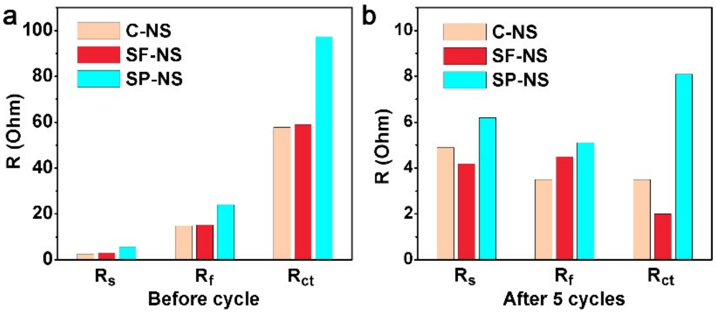

Fig. S9. The comparison of resistance during C-NS, SF-NS and SP-NS before (a) and after 5 cycles (b).

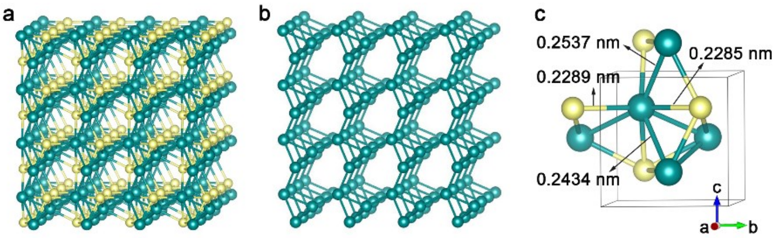

Fig. S10. (a) The crystal structure of Ni_3S_2. (b) The continuous network of Ni-Ni bonds in Ni_3S_2. (c) The triangular bipyramids structure in Ni_3S_2 and the bond lengths.

Ni_3S_2 possesses a rhombohedral structure, which belongs to the space group R32 with lattice constants a=b=c=0.4082 nm and α=β=γ=89.475°. The structure comprises a series of interconnected Ni_3S_2 triangular bipyramids composed of Ni_3 triangles and apical S atoms those are connected by Ni-S bonds and Ni-Ni bonds (Fig. S10a). The interconnected Ni_3 triangles form a continuous network of Ni-Ni bonds (Fig. S10b), which is advantageous for the transport of electron in Ni_3S_2. The Ni-Ni/Ni-S bond lengths inner and outer the bipyramids are 0.2434/0.2285 and 0.2537/0.2289 nm (Fig. S10c), respectively

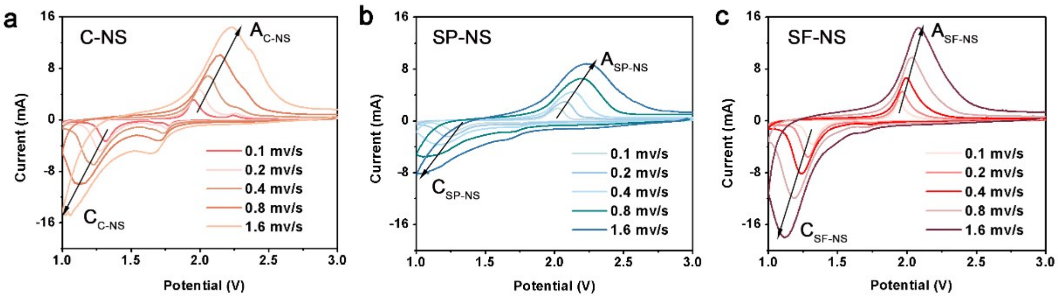

Fig. S11. The CV curves of (a) C-NS, (b) SP-NS and (c) SF-NS recorded at the scan rate from 0.1 to 1.6 mV s^{-1} between 1.0 and 3.0 V.

Table S1. Comprision of synthesis routes and capacity retention between present and previously work

Cathodes	**Capacity retention**	**Cycle numbers**	**Current density**	**Synthesis methods**	**Synthesis periods**	**Solvent-free**
Ni_3S_2/Ni particles on carbon fibers web[1]	65%	30	100 mA/g	Wet chemistry method	＞24h	No
3D porous Ni_3S_2[2]	105%	55	150 mA/g	Solvothermal method	12h	No
Ni_3S_2 nanoplates on Ni foam[3]	89%	150	100 mA/g	Hydrothermal method	7.5h	No
Ni_3S_2@N-doped carbon nanowires arrays[4]	91%	100	1000 mA/g	Chemical vapor deposition	1h	Yes
Ni_3S_2 nanobowls-rGO composites[5]	74%	500	231 mA/g	Wet chemistry method	＞5.5h	No
Ni_3S_2@CNT paper[6]	87%	100	300 mA/g	Electrodeposition method	＞24h	No
Ni_3S_2 nanocrystals embed in hollow carbon fibers[7]	56%	100	100 mA/g	Bioleaching strategy	＞6 days	No
Ni_3S_2 nanoparticles encapsulated in interconnected N-doped porous carbon[8]	122%	100	100 mA/g	Freeze-drying and in-situ conversion	＞2days	No
Ni_3S_2@C/RGO[9]	80%	80	200 mA/g	Wet chemistry method	＞11h	No
Stone-forest-like nickel sulfides [This work]	93%	100	500 mA/g	One-pot plasma sulfidation reaction	6 min	Yes

References

1. D. K. Lee, C. W. Ahn and H.-J. Jeon, *Microelectron. Eng.*, 2016, **166**, 1-4.
2. J. Zhu and G. Hu, *Mater. Lett.*, 2016, **166**, 307-310.
3. Z. Zhang, H. Zhao, Q. Xia, J. Allen, Z. Zeng, C. Gao, Z. Li, X. Du and K. Świerczek, *Electrochim. Acta*, 2016, **211**, 761-767.
4. Z. Yao, L. Zhou, H. Yin, X. Wang, D. Xie, X. Xia, C. Gu and J. Tu, *Small*, 2019, **15**, e1904433.
5. W. Zhou, J.-L. Zheng, Y.-H. Yue and L. Guo, *Nano Energy*, 2015, **11**, 428-435.
6. P. Fan, H. Liu, L. Liao, J. Fu, Z. Wang, G. Lv, L. Mei, H. Hao, J. Xing and J. Dong, *RSC Adv.*, 2017, **7**, 49739-49744.
7. J. Li, J. Cao, X. Li, H. M. K. Sari, L. Li, C. Lv, I. V. Zatovsky and W. Han, *Electrochim. Acta*, 2020, **332**, 135446.
8. J. Li, J. Li, Z. Ding, X. Zhang, Y. Li, T. Lu, Y. Yao, W. Mai and L. Pan, *Chem. Eng. J.*, 2019, **378**, 122108.
9. I. A. Khan, R. Medwal, S. Fareed, A. Farid, J. V. Vas, M. V. Reddy and R. S. Rawat, *Mater. Res. Express*, 2020, **7**, 015517.